# The Heterogeneous Reaction of NO 2 with NH 4 Cl: A Molecular Diffusion Tube Study

**ARTICLE** *in* JOURNAL OF ATMOSPHERIC CHEMISTRY · FEBRUARY 2005

Impact Factor: 1.95 · DOI: 10.1007/s10874-005-5898-4



**2 AUTHORS**, INCLUDING:

Michel J Rossi
Paul Scherrer Institut
**259** PUBLICATIONS **6,466** CITATIONS

SEE PROFILE

Journal of Atmospheric Chemistry (2005) 50: 171–194
DOI: 10.1007/s10874-005-5898-4 

# The Heterogeneous Reaction of $NO_2$ with $NH_4Cl$: A Molecular Diffusion Tube Study

NORIMICHI TAKENAKA[1] and MICHEL J. ROSSI[2]

[1]*Laboratory of Environmental Chemistry, Department of Applied Materials Science, Graduate School of Engineering, Osaka Prefecture University, Gakuen-cho 1-1, Sakai, Osaka, 599-8531, Japan, e-mail: takenaka@ams.osakafu-u.ac.jp*
[2]*Laboratoire de Pollution Atmosphérique et Sol (LPAS), Faculté Environnement Naturel, Construit et Architectural (ENAC), Ecole Polytechnique Fédérale de Lausanne (EPFL), CH-1015 Lausanne, Switzerland*

(Received: 26 August 2003; accepted: 19 July 2004)

**Abstract.** The heterogeneous interaction of nitrogen dioxide with ammonium chloride was investigated in a molecular diffusion tube experiment at 295–335 K and interpreted using Monte Carlo trajectory calculations. The surface residence time ($\tau_{surf}$) of $NO_2$ on $NH_4Cl$ is equal to 15 $\mu$s at 295 K, increases with temperature up to 323 K ($\tau_{surf} = 45$ $\mu$s) and probably decreases beyond 323 K. The same experiment also yields uptake coefficients, $\gamma$, which are derived from the absolute number of surviving molecules effusing out of the diffusion tube. The rate of uptake of $NO_2$ on $NH_4Cl$ followed a rate law first order in [$NO_2$] and the uptake coefficient $\gamma$ is equal to $7 \times 10^{-5}$ at 295 K, increases with temperature up to 323 K ($\gamma = 2.1 \times 10^{-4}$) and probably decreases beyond 323 K. Nitrous acid, water and nitrogen were detected as products. From these products, it is concluded that the reaction of $NO_2$ with $NH_4Cl$ is a reverse disproportionation reaction where two moles of $NO_2$ result in ammonium nitrite, $NH_4NO_2$, as an intermediate, and nitryl chloride, $NO_2Cl$. $NH_4NO_2$ decomposes in two pathways, one to nitrous acid, HONO and $NH_3$, the other to nitrogen and water. The branching ratio for the production of HONO + $NH_3$ to that of $N_2 + H_2O$ is approximately 20 at 298 K and increases with increasing temperature.

**Key words:** molecular diffusion tube, nitrogen dioxide, ammonium salts, nitrous acid, uptake coefficient, tropospheric aerosols

## 1. Introduction

Nitrogen dioxide is one of the key compounds in atmospheric chemistry as it catalyzes both tropospheric ozone formation as well as ozone destruction processes. Therefore, the sources and sinks of $NO_2$ are of great interest as they determine its atmospheric concentrations and thus the rate of ozone formation and destruction. Recently, there has been great interest in the heterogeneous reactions of nitrogen dioxide interacting with atmospheric particulates (Vogt and Finlayson, 1994; Tabor *et al.*, 1994; Ammann, 1998; Longfellow *et al.*, 1999; Weis and Ewing, 1999; Grassian, 2001; Underwood *et al.*, 2001). A measure of the heterogeneous interaction of $NO_2$ with atmospheric particulates is the uptake coefficient $\gamma$, which is

the probability per collision that $NO_2$ is irreversibly removed from the gas phase on the time scale of the experiment. It ranges from very low, typically on the order of a few $10^{-7}$ for the reaction of $NO_2$ with salts (Fenter *et al.*, 1997a) to the few percent range ($10^{-2}$) or even higher for the interaction of $NO_2$ with soot (Tabor *et al.*, 1994; Ammann, 1998; Rossi, 2003).

This work explores the potential heterogeneous interaction in terms of uptake kinetics of $NO_2$ on ammonium salts and reaction products resulting from such a reaction. One should take note of the fact that ammonium salts such as $NH_4NO_3$, $NH_4HSO_4$, $(NH_4)_2SO_4$ and $NH_4Cl$ represent reduced nitrogen in its oxidation state (−III) whereas $NO_2$ represents oxidized nitrogen in its (+IV) state. We, therefore, have explored the possibility whether or not a reverse heterogeneous disproportionation reaction or internal oxidation–reduction reaction may occur under atmospheric conditions using $NH_4Cl$ as a proxy of an ammonium salt occurring in tropospheric aerosols.

Ammonia is released from the ground to the atmosphere from both natural as well as from anthropogenic sources, especially owing to the decomposition of urine in areas with an intense livestock activity, and from exhaust gases emitted from vehicles equipped with a three-way catalyst (Bouwman *et al.*, 1997; Fraser and Cass, 1998; Baum, 2001). Only recently, research has developed promising experimental methods at measuring atmospheric concentrations of ammonia in a reliable and reproducible manner (Fehsenfeld *et al.*, 2002). Owing to the acidity of the atmosphere ammonia readily reacts with atmospheric acidity such as $HNO_3$, HCl, and $H_2SO_4$ to produce atmospheric particulates of ammonium salts (Seinfeld and Pandis, 1998). These occur in a characteristic vertical distribution whose maximum is located in the planetary boundary layer and which steadily decreases with altitude. Concomitantly, the acidity of the lower troposphere continuously increases with altitude as $NH_3$ is the most common basic gas counteracting atmospheric acidity. Concentrations of $NH_4Cl$ and $(NH_4)_2SO_4$ are in the sub $\mu g\ m^{-3}$ range and that of $NH_4NO_3$ is less than $10^{-2}$ $\mu g\ m^{-3}$ close to the ground (Jacobson, 2001). The $NH_4Cl$ concentration usually decreases with increasing altitude. At low altitude the most common ammonium salt is $(NH_4)_2SO_4$ turning over to the more acidic $NH_4HSO_4$ at higher altitude. Finally, the $NH_3$ concentration in the upper troposphere and lower stratosphere is vanishing so that sulfate occurs as $H_2SO_4$ droplets. Similarly, $NH_4NO_3$ is found close to the planetary boundary layer, with $HNO_3$ being present higher up. However, even at altitudes of the free troposphere the nitrate is still fully neutralized and occurs as $NH_4NO_3$. However, $NH_4^+$ ions represent on average close to 50% of the total water-soluble mass fraction in the aerosol fine fraction characterized by PM1 (Henning *et al.*, 2003). On the other hand, the $NH_4^+$ mass fraction is less than 10% in the coarse aerosol fraction under conditions where aerosol mass closure has been achieved up to 70% (Puteaud *et al.*, 2002). Amines are well known to interact strongly with $NO_2$ (Levaggi *et al.*, 1973; Huygen, 1971; Finlayson and Pitts, 1999). However, the interaction of $NO_2$ with ammonium salts in the atmosphere has to our knowledge neither been considered nor been investigated so far. In addition, there

seem to be industrial applications involving the formation of ammonium salts in relation to flue gas clean-up. It was determined that ammonium salt aerosols substantially enhanced total $NO_x$ removal when ozone, $SO_2$ and $NH_3$ were added to flue gas from combustion processes regardless of the molecular processes involved (Tseng and Keener, 2001; van Veldhuizen *et al.*, 1998). Moreover, ammonium salts seem to have a small but significant positive radiative forcing that will contribute to global warming (Jacobson, 2001).

The molecular diffusion tube technique has recently been developed and has been used for measurements of uptake coefficients and surface residence times of adsorbed gas molecule on salt and soot substrates (Koch and Rossi, 1998; Koch *et al.*, 1997, 1999; Alcala and Rossi, 2000; Alcala *et al.*, 2002). This method is able to sample a very wide range of collision numbers for gases interacting with the substrates of interest depending on the ratio of the diameter to length of the chosen diffusion tube. The method excels at the measurement of low reaction probabilities and long surface residence times, with typical values of $\gamma$ being in the range $10^{-3}$ to $10^{-6}$ and $\tau_{surf}$ ranging from a few $\mu$s to a few hundred ms. The interest in both parameters, namely $\gamma$ and $\tau_{surf}$ stems from the fact that there seems to exist a 1:1 correspondence between the surface residence time and the reaction probability following the Langmuir–Hinshelwood mechanism for obvious reasons (Koch *et al.*, 1999): A long surface residence time, that is a small rate of desorption, gives rise to an increased probability for surface reaction if we allow the molecule to look for an active reaction site according to the Langmuir–Hinshelwood mechanism which excludes direct collisions of the gas with the active surface site. We report here the uptake coefficient, surface residence time and products of the reaction of $NO_2$ with ammonium chloride by using the molecular diffusion tube experiment.

## 2. Experimental

The experimental apparatus used in the present study corresponds to the same configuration as used by Koch and Rossi (1998) and Koch *et al.* (1997, 1999) except for some changes in the dimension of the diffusion tube and the detection chamber. The dimension of the diffusion tubes used throughout is 1.15 cm inner diameter and 100 cm length, and that of the detection chamber is 10 cm in diameter and 34 cm in length. The diffusion tubes are made out of Pyrex glass and were used in pairs, that is, one tube was coated with ammonium chloride as the sample tube, whereas the other was coated with FEP 120-A (tetrafluoroethylene-hexafluoro propylene copolymer kindly provided by Mr. Danilevi of Dupont SA, Geneva) as the reference tube.

### 2.1. METHOD OF SUBSTRATE PREPARATION

A saturated solution of $NH_4Cl$ in methanol was sprayed across a 40 cm long nozzle atomizer onto the inside surface of a heated glass tube (383 K) serving as the

diffusion tube. The long nozzle atomizer consists of two concentric tubes, one for the air flow and the other for the solution whose solute was to be atomized. The principle of this atomizer is identical to that of a commercial underpressure type atomizer. Multiple coatings were applied by spraying from both ends of the tube. Finally, the coated tube was dried at 383 K for several tens of minutes. The total quantity of $NH_4Cl$ used for coating was between 0.8 and 1.7 mg $cm^{-2}$. The reference tube was coated with the FEP suspension using the same atomizer. Before the FEP aqueous solution was sprayed onto the Pyrex tube it was filled to the brim with a 10% HF aqueous solution in order to superficially etch the glass for 30 min. It was then washed several times with distilled water. After mixing one volume of the FEP emulsion with four volumes of water the mixed solution was sprayed onto the inside of the tube that was heated to 423 K. After spraying the tube was heated to 553 K for 2 h and to 653 K for 1 h for curing before being mounted onto the vacuum chamber.

An aqueous salt solution was also sprayed using the long nozzle atomizer. In this case, the coating was not very uniform if a saturated salt solution was used. Also, if the spraying was continued for longer than 3–5 s, water vapor was deposited on the portion of the tube already coated and negatively affected the quality of the coating in that the salt deposit formed islands. Therefore, dilute salt solutions were used and repeatedly sprayed for a short time in one coating session.

The diffusion tube was also coated with ammonium chloride using the gas phase neutralization reaction of ammonia with hydrochloric acid. Nitrogen was bubbled into vessels of concentrated aqueous solutions of ammonia and hydrochloric acid, respectively, and the combined air flows containing gaseous ammonia and HCl were introduced into the diffusion tube. The ammonium chloride was produced in the gas-phase as an aerosol and subsequently deposited onto the inside walls of the diffusion tube. The tube was finally heated to 383 K in order to remove water that was adsorbed on the thin salt films. The quantity of $NH_4Cl$ aerosol used to coat the tube was 0.6–1.5 mg $cm^{-2}$.

### 2.2. CHEMICALS

Nitrogen dioxide was prepared and purified as follows: $NO_2$ was mixed with pure oxygen in a glass vessel and was left for several hours to oxidize the impurity NO to $NO_2$. $NO_2$ and $O_2$ were dried by passage across a $P_2O_5$-filled trap before mixing. The vessel was cooled down to 77 K and evacuated for approximately 20 min. The sample was subsequently heated to ambient temperature. This freeze-pump-thaw process was repeated 3 to 4 times.

The remaining gases were commercially available and were used without further purification. Nitrous acid, HONO, was generated in the reaction of $KNO_2$ with HCl gas, which was produced from the reaction of crystalline NaCl with concentrated $H_2SO_4$. The sample included $NO_2$, NO and $H_2O$ owing to either heterogeneous or condensed phase decomposition of HONO. Therefore, the quantitative assessment

of the HONO concentration was performed by taking into account the quantity of the impurity molecules $NO_2$, NO and $H_2O$ in metering the flow rate of the HONO source gas. All reagents were obtained from Fluka AG and used without further purification.

### 2.3. EXPERIMENTAL PROCEDURE

The FEP coated (reference) and $NH_4Cl$ coated tubes were both mounted on the detection chamber and capped with two pulsed solenoid valves of 2 mm diameter orifice (IOTA One System, General Valve Inc.). Nitrogen dioxide was introduced into a glass storage vessel of known volume, which was connected to the pulsed solenoid valves. The pressure of $NO_2$ within the calibrated vessel was adjusted to 0.2–0.5 Torr, and the vessel was covered with aluminum foil to prevent photolysis of $NO_2$. A quantity of approximately $4 \times 10^{14}$ molecules of $NO_2$ were alternately pulsed into the reference or sample tube, and the time profiles of the MS signals of the effusing $NO_2$ and product molecules such as HONO, $N_2$ and $H_2O$ were monitored using a Balzers QMS 422 Mass Spectrometer controlled by Quadstar software. The obtained MS signal was transferred to a PC and both the area under the MS signal as well as its decay rate was analyzed.

The comparison of the $NO_2$ data with the signals obtained using Ar provided the baseline for the reactivity of $NO_2$ in view of the very similar molecular masses involved. This comparison has been performed both for the $NH_4Cl$- and FEP-coated tube in order to check for the effect of the polycrystalline nature of the salt coating with respect to the smooth FEP coating for both the non-reactive (Ar) as well as the reactive case ($NO_2$). Several reasons may lead to quantitative differences in the raw MS signals corresponding to the arrival time of a non-interacting gas diffusing across the smooth FEP tube vs. the sample tube coated with a rough salt film. Specifically, the roughness of the salt film owing to its polycrystalline nature as well as a usually small difference in internal diameter between the coated sample and reference tube lead to an approximately 5% longer arrival time for Ar diffusing across the $NH_4Cl$-coated tube. However, there are small day-to-day changes of the same magnitude (say a few %) because of differences in the morphology of the salt coating. In addition, small differences in the length of the opening times of the two different pulsed solenoid valves lead to differences in the applied doses when comparing sample and reference tube. In order to enable simple comparison of small differences in the thickness between sample and reference coatings we used Ar as a non-interacting probe by measuring the arrival time of Ar for both the sample and the reference tubes. We, thereby, scaled both the decay as well as the dose with respect to Ar in order to put both the raw time-dependent MS signals for the sample and the reference tube onto a common basis.

The partial pressure of $NO_2$ in the calibrated vessel was in the range 0.2–0.5 Torr. Under these conditions the percentage of $N_2O_4$ in $NO_2$ was less than 0.4 percent at 298 K using the published equilibrium constant (DeMore *et al.*, 1997).

The contribution of $N_2O_4$ relative to $NO_2$ is negligible in the diffusion tube as well as in the detection chamber whose background pressure during the experiment was of the order of $10^{-7}$ Torr or less. In addition, the rate constant for dissociation of $N_2O_4$ into $2NO_2$ is in the limiting low-pressure regime and is estimated at a limiting low value of 5 $s^{-1}$ which would be roughly ten times faster than the inverse of the expected arrival time of $N_2O_4$ based on kinetic experiments (Markwalder *et al.*, 1992). Even in the case of a significant equilibrium fraction of $N_2O_4$ in $NO_2$ its dissociation would occur on a time scale faster than $NO_2$ effusion and would not affect the experimental results for $NO_2$.

Standard experimental conditions prevail when using the methanol salt solution spray coating for the sample diffusion tube and doses of (4–5) $\times 10^{14}$ $NO_2$ molecules per individual pulse. Experiments performed at doses of $4 \times 10^{15}$ per pulse are called "large dose" experiments. Experiments whose dose was in the range (4–5) $\times 10^{14}$ per pulse in conjunction with the use of aqueous salt solution spray coatings and coatings prepared by $NH_4Cl$ aerosol deposition are labeled "aqueous solution coating" and "gas phase reaction" experiments, respectively.

### 2.4. MONTE CARLO SIMULATION

The simulation used in this study is based on a Monte Carlo trajectory model that has been developed by Fenter *et al.* (1997b) and that has been designed to investigate the effect of the geometry of the Knudsen cell on the gas dynamics within the reactor. Briefly, the program calculates the trajectories of individual molecules injected into a given reactor geometry on the assumption that the molecules are reflected according to a cosine directional distribution function upon collision with the wall surface. The cosine law even applies to microscopically rough surfaces under the condition that it describes the behavior of the average molecule, that is for a sufficient number of molecular trajectories. A given experimental situation is simulated by the superposition of typically $10^4$ to $10^5$ trajectories. The details of the computer code that also includes chemical reactivity expressed as an uptake coefficient of the gas by the substrate are described in Fenter *et al.* (1997b), Koch and Rossi (1998), Koch *et al.* (1997, 1999), Alcala *et al.* (2002) and Alcala and Rossi (2000, 2004).

## 3. Results and Discussion

### 3.1. RELATIONSHIP BETWEEN THE GEOMETRY OF THE DIFFUSION TUBE AND THE ARRIVAL TIME $\tau$

Figure 1 shows an example of a time profile of a raw MS signal corresponding to a pulse of $NO_2$ molecules diffusing across both a FEP- and $NH_4Cl$-coated diffusion tube of nominally equal geometry. The $NO_2$ is introduced in repetitive pulses of approximately $10^{14}$ to $10^{15}$ molecules per pulse, and the average molecule collides

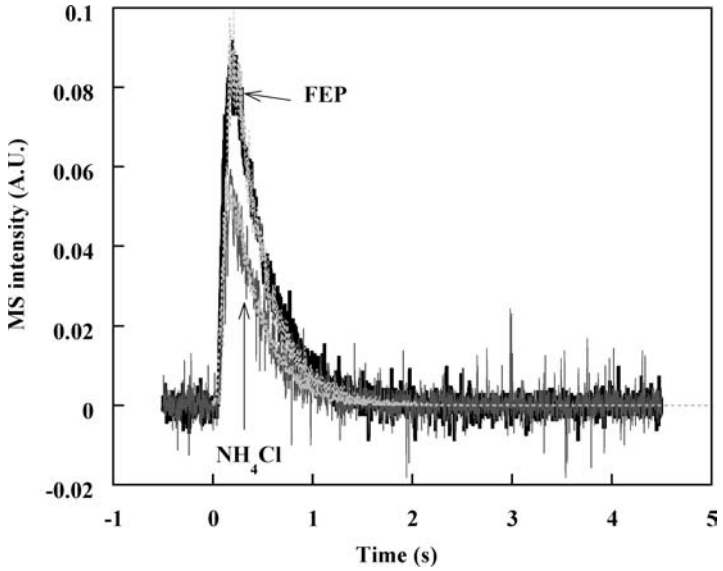


*Figure 1.* Trace of mass spectrometer signal recorded at m/e = 46 and its Monte Carlo simulation for the interaction of $NO_2$ with the $NH_4Cl$ coated tube. Black trace; mass spectrometer signal for $NO_2$ on FEP. Gray trace; mass spectrometer signal for $NO_2$ on $NH_4Cl$. Gray dotted traces; Monte Carlo simulations for $NO_2$ on FEP and on $NH_4Cl$. The diameter (id) and length of the diffusion tube are 1.15 and 100 cm, respectively. Those for the detection chamber housing the mass spectrometer are 34 and 10 cm, respectively. The calculated collision number is 11,000.

11,000 times with the internal wall before escaping into the MS detection chamber. The collision number, which is the number of collisions undergone by an average $NO_2$ molecule during its gas phase residence time that is given by the arrival time of $NO_2$ diffusing across the non-interactive FEP-coated tube has been calculated using the Monte-Carlo trajectory code. It is noted that the temporal time profiles of the MS signal (arrival time spectrum) of both non-interactive and interactive, albeit non-reactive molecular probes follow an exponential decay in agreement with Monte Carlo simulations (Koch and Rossi, 1998; Koch *et al.*, 1999; Alcala and Rossi, 2000, 2004) whose first-order decay rate constant $k$ is related to the arrival time $\tau$ ($k = 1/\tau$). In keeping with prior use we characterize a substrate-probe molecule pair by "non-interactive" and "interactive". The adsorption behavior of both groups of molecules is distinctly different according to whether or not a surface residence time $\tau_{surf}$ may be observed. As has been explained in the literature $\tau_{surf}$ is given by the increase of the arrival time $\tau$ with respect to a reference that represents a non-interactive pair most often involving rare gases and rare gas-like molecules. A non-reactive and reactive substrate–molecule pair is a subgroup of the interactive pair depending on whether or not reaction products are observed. Therefore, it is possible to have an interactive pair that is non-reactive, for instance the system $H_2O$-soot (Alcala *et al.*, 2002; Alcala and Rossi, 2004).

In the absence of sticky collisions of $NO_2$ with the internal walls of the diffusion tube this arrival time $\tau$ only addresses the net flight time across the gas phase which is a function of the geometry of the tube as well as the mass and temperature of the probe molecule. The inverse of the decay rate constant $k$ corresponds therefore to the lifetime of the probe gas molecules in the diffusion tube. In the case of "sticky" collisions of the probe with the coating of interest within the internal walls of the diffusion tube $\tau$ increases compared to a non-interactive situation observed on a FEP coating. The difference between the sample and reference arrival times is attributed to the surface residence time $\tau_{\text{surf}}$ that is expressed on a per collision basis. The incidence of a heterogeneous chemical reaction on the surface of the (reactive) coating leads to a non-exponential shape of the arrival time spectrum such that curve fitting using two parameters, namely $\tau_{\text{surf}}$ and $\gamma$, the latter of which corresponds to the uptake coefficient on a per collision basis, has to be performed using the Monte-Carlo trajectory code (Koch and Rossi, 1998; Koch *et al.*, 1999; Alcala and Rossi, 2000). One may note the crucial importance of the arrival time of M in the reference tube corresponding to the lifetime of M in the non-interacting diffusion tube against which the surface residence time $\tau_{\text{surf}}$ is measured. We have established that the absolute arrival time of $NO_2$ in the FEP-coated diffusion tube perfectly matches the calculated one using the Monte Carlo trajectory code that only uses the geometry of the tube as well as the temperature and mass of the colliding molecule as input parameters.

The arrival time $\tau$ is calculated by dividing the trajectory $L$ of the average gas molecule M by the average molecular velocity of M, $\bar{v}$ according to equation (1).

$$\frac{1}{k} = \tau = \frac{L}{\bar{v}} = L\sqrt{\frac{\pi m}{8k_{\text{B}}T}} \tag{1}$$

Here, $k_{\text{B}}$ is the Boltzmann constant, $T$ the absolute temperature, and $m$ the mass of M. The arrival time of non-interacting gases is proportional to the square root of $m$, the molecular mass of M as shown in Figure 2 that shows a linear correlation between the arrival time $\tau$ or $1/k$ and the square root of $m$ of He, Ne, $N_2$, Ar, and $SF_6$. The slope of the straight line going through the origin and displayed in Figure 2 corresponds to $L\sqrt{\frac{\pi}{8k_{\text{B}}T}}$. The total length $L$ of the average molecular trajectory after 11,000 collisions across the given diffusion tube was calculated to be 120 m at 298 K independent of the mass of M. This leads to an average distance of 1.1 cm between collisions that correspond to the diameter of the used diffusion tube. This result is expected because the most probable trajectory of the average molecule is normal to the tube axis along the tube diameter. The mean free path of $NO_2$ is estimated to be 480 m at 298 K and $10^{-7}$ Torr using 3.8 Å as a hard sphere collision diameter for $N_2$ and is commensurate with the absence of any gas–gas collisions in the diffusion tube in agreement with the requirement of free molecular flow.

The present case of the interaction of $NO_2$ with solid ammonium salts represents an interactive system which may be described by two adjustable parameters as a minimum requirement: the surface residence time $\tau_{\text{surf}}$ of $NO_2$ and the uptake

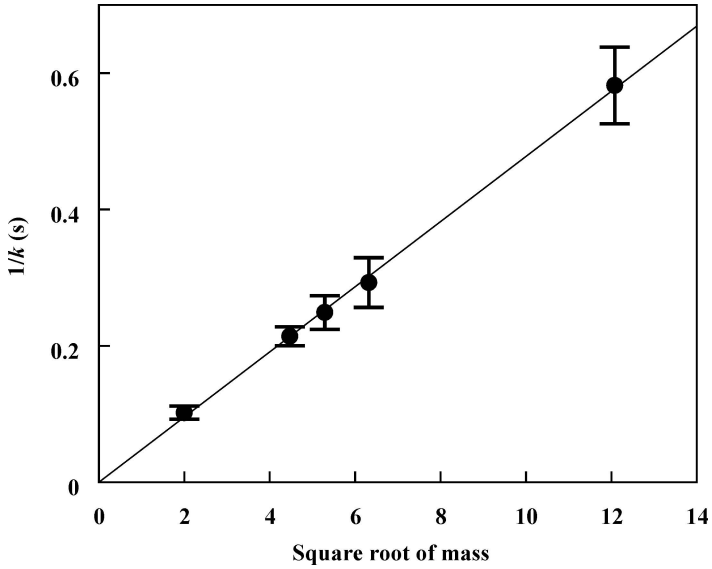


*Figure 2.* Calibration plot of experimental arrival time of ideal gases (He, Ne, $N_2$, Ar and $SF_6$) effusing out of the $NH_4Cl$-coated tube (1.15 cm i.d., 100 cm length) at 298 K. $1/k = 4.78 \times 10^{-2}$ (molecular mass)$^{1/2} + 5.2 \times 10^{-4}$, The correlation coefficient is 0.9994. The error bars indicate 1 standard deviation of 5 data.

coefficient $\gamma$ which describes the irreversible removal probability of $NO_2$ from the gas phase, both of which have been obtained from the experimental arrival time spectra ($\tau_{\text{surf}}$) as well as from its integral ($\gamma$) displayed in Figure 1. The reactivity given by $\gamma$ and the surface residence time $\tau_{\text{surf}}$ affect both the temporal shape as well as the area under the raw MS signal because fewer molecules effuse owing to chemical reaction. In addition, the distribution of effusing molecules at long elapsed time is curtailed because the molecules undergoing a large number of collisions are the ones that are preferentially removed owing to chemical reaction. This phenomenon is one of the reasons for the non-exponential behavior of the MS signal. Figure 1 presents experimental and simulated arrival time spectra based on raw MS signals that have been obtained using the above-mentioned two parameters that act against each other. In all cases we have obtained excellent agreement between experimental and simulated MS signals using only the two parameters, $\tau_{\text{surf}}$ and $\gamma$.

### 3.2. THE SURFACE RESIDENCE TIME $\tau_{\text{surf}}$ AND THE UPTAKE COEFFICIENT $\gamma$

In order to present the relationship between the measured or fitted parameters and the rate coefficients of the interacting substrate–molecule pair we will consider a simplified interaction scheme as follows:

$$NO_2(g) \underset{k_d}{\overset{k_a}{\rightleftharpoons}} NO_2(ads) \xrightarrow{k_r} \text{Products} \qquad (2)$$

where $k_a$, $k_d$ and $k_r$ are the rate constants for adsorption, desorption and surface reaction of $NO_2$. A convenient normalization for $k_a$ obtains $\gamma$, the uptake coefficient, using $\gamma = k_a/\omega$ where $\omega$ is the gas-substrate collision frequency. The uptake coefficient $\gamma$ corresponds to the probability for $NO_2$ disappearing from the gas phase regardless of the subsequent fate of $NO_2$(ads). The surface residence time $\tau_{surf}$ describes the kinetics of desorption of the adsorbed molecule according to $\tau_{surf} = 1/(k_d + k_r)$ which reduces to $1/k_d$ in the absence of surface reaction. Therefore, $\tau_{surf}$ and $\gamma$ are complementary in nature and completely determine the system either in equilibrium or in steady state depending on whether a surface chemical reaction occurs or not. The experimental method used here affords the possibility to separately determine or decouple the kinetic parameters from a fundamental point of view (Boudart and Djéga-Mariadassou, 1984).

The surface residence time $\tau_{surf}$ provides information on those molecules that did not react during the interaction time and, therefore, survived the heterogeneous interaction unscathed, whereas the uptake coefficient describes that fraction of molecules that disappears from the gas phase by either staying adsorbed on the solid substrate (interactive case) or undergoing a heterogeneous reaction (reactive case). These two observables are, therefore, highly complementary and should yield information about the reaction mechanism. Figure 3 displays the sensitivity of hypothetical (calculated) arrival time spectra of $NO_2$ interacting with solid $NH_4Cl$ as a function of $\tau_{surf}$. The Monte Carlo simulation reveals that at the chosen geometry surface residence times larger than 1 $\mu$s may be fitted to experimental arrival time

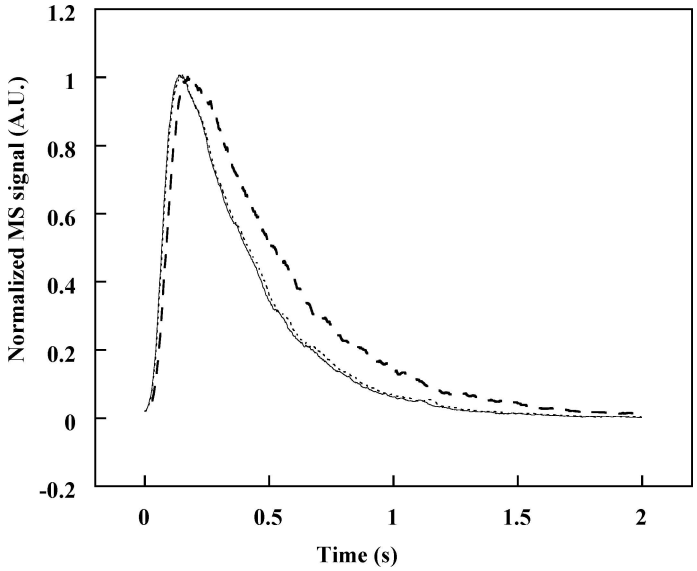


*Figure 3.* Monte Carlo simulations of the $NO_2$ MS signal at several surface residence times $\tau_{surf}$ for the case of no reaction of $NO_2$ with $NH_4Cl$ ($\gamma = 0$). Surface residence time $\tau_{surf}$: solid line; 0 $\mu$s, dotted line; 1 $\mu$s, broken line; 10 $\mu$s.

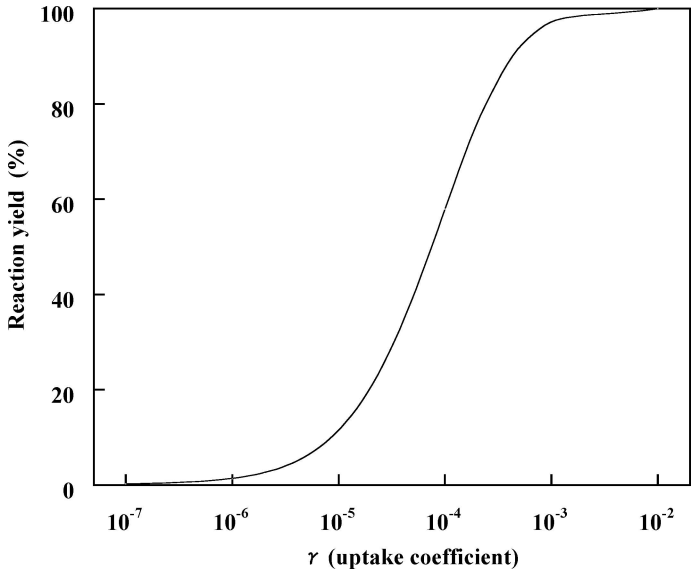


*Figure 4.* The relation between the reaction yield Y and the uptake coefficient $\gamma$ for a $NH_4Cl$ coated tube of 1.15 cm id $\times$ 100 cm at 298 K.

spectra as they significantly influence the shape of the decaying portion of the arrival time spectrum, whereas values of $\tau_{surf} < 1$ $\mu$s do not noticeably influence the MS signals. In this particular case the fitting has been performed using the decaying portion of the arrival time spectrum as values of $\tau_{surf} < 10$ $\mu$s only have a small effect on the rising portion of the MS signal as displayed in Figure 3. Figure 4 shows the relationship between the uptake coefficient $\gamma$ and the reaction yield that is based on the relative decrease in area under the time dependent MS signal for the $NH_4Cl$-coated tube relative to the non-reactive case where $NO_2$ diffuses across a FEP-coated tube (see Figure 1). Using a tube of 1.15 cm inner diameter and 100 cm length uptake coefficients in the range $10^{-3}$ to $10^{-6}$ can conveniently be measured. This means that reaction yields in the range 3–97% will have to be measured which is equal to the measurement accuracy of the present method. One has to take note of the fact that in general both parameters have to be found simultaneously by fitting to experimental arrival time spectra. This is enabled by the Monte Carlo trajectory code that treats both processes simultaneously. However, for small values of $\gamma$ as measured in the present study the mutual interaction of both fitting parameters, $\tau_{surf}$ and $\gamma$, in regards to the arrival time spectrum is negligible. Therefore, $\gamma$ has been evaluated from the number of surviving, that is effusing $NO_2$ molecules using Figure 4 as a nomograph so that only a single parameter ($\tau_{surf}$) has been fitted to the arrival time of $NO_2$.

Table I presents the dose, that is the number of molecules of $NO_2$ per pulse introduced into the diffusion tube and the percentage of surviving $NO_2$ molecules effusing out of the tube as well as the resulting uptake coefficients obtained by

*Table I.* Summary of results for the interaction of $NO_2$ on solid $NH_4Cl$

| Temperature (K) | Number ($\times 10^{14}$) | Number out (%) | $1/k$ (s) | $\gamma$ ($\times 10^{-5}$) | $\tau_{surf}$ ($\mu$s) | [a] | No.[b] |
|---|---|---|---|---|---|---|---|
| 295 | 4 | 47.3 | 0.31 | 7 | 15 | | 1 |
| 298 | 4 | $55.0 \pm 5.6$ | $0.33 \pm 0.05$ | $6 \pm 1.2$ | $16 \pm 7$ | | 9 |
| 298 | 40 | $46.4 \pm 13.0$ | $0.28 \pm 0.02$ | $8 \pm 3.8$ | $15 \pm 5$ | Large dose | 3 |
| 298 | 4 | $87.6 \pm 3.6$ | $0.36 \pm 0.01$ | $1 \pm 0.3$ | $6 \pm 2$ | Gas prep. | 5 |
| 300 | 4 | $48.2 \pm 10.3$ | $0.43 \pm 0.07$ | $7 \pm 2.3$ | $28 \pm 8$ | Aq. soln. | 6 |
| 312 | 5 | $22.3 \pm 4.2$ | $0.56 \pm 0.17$ | $20 \pm 4$ | $33 \pm 6$ | | 3 |
| 323 | 5 | 19.6 | 0.53 | 21 | 45 | | 1 |
| 335 | 5 | $32.3 \pm 5.2$ | $0.35 \pm 0.01$ | $13 \pm 3$ | $40 \pm 14$ | | 2 |

[a]"Large dose" corresponds to approximately $4 \times 10^{15}$ molecule/pulse, the remaining standard runs correspond to approximately $4 \times 10^{14}$ molecule/pulse using saturated $CH_3OH$ salt solutions for spray application; "Gas prep." corresponds to deposition of $NH_4Cl$ aerosol from the gas phase reaction of HCl with $NH_3$; "Aq. soln." corresponds to the spray application of an aqueous $NH_4Cl$ solution.

[b]Each data were obtained as an average of three pulses. The rightmost column (No) corresponds to the number of experiments each using a new coating.

Monte Carlo simulation. The first column on the right of Table I indicates the number of independent experiments performed, each on a fresh $NH_4Cl$ coating as Table I presents the average values of the measured kinetic parameters. For a given coating saturation phenomena are observed with increasing number of $NO_2$ pulses that will be discussed below. For large doses the experiment was performed in single shot whereas for standard or low $NO_2$ doses in the range $10^{14}$–$10^{15}$ molecules the first three arrival time spectra were averaged in order to improve the signal/noise ratio of the raw MS signals. Noteworthy is the small albeit significant uptake coefficient observed over the whole temperature range that has to our knowledge never been observed before. It needs to be pointed out that the uptake coefficient resulting from the measured number of surviving $NO_2$ molecules is independent of the dose of $NO_2$ used within experimental uncertainty. This leads to the conclusion that the corresponding rate coefficient $k_a$ for $NO_2$ uptake is first order in $[NO_2]$ for a given substrate preparation protocol. In addition, Table I also shows the experimental decay rate constants of the time-dependent MS signal corresponding to the fitted surface residence times $\tau_{surf}$. Figures 5 and 6 show the temperature dependence of the surface residence time $\tau_{surf}$ and of the uptake coefficient $\gamma$, respectively. A typical value of $\tau_{surf} = 16 \pm 7$ $\mu$s has been obtained at 298 K which increases with increasing temperature up to 323 K and seems to decrease beyond. Similarly, $\gamma$ has positive temperature dependence from ambient to 323 K beyond which it seems to decrease as displayed in Figure 6. Figure 6 shows the dependence of $\gamma$ on temperature starting with a value of $(6 \pm 1) \times 10^{-5}$ at 298 K. This value is larger by two-to-three orders of magnitude compared to that for the heterogeneous reaction

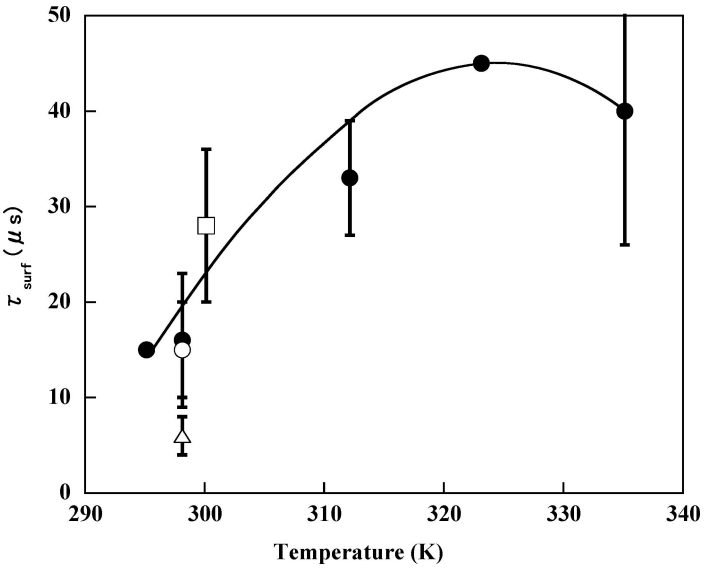


*Figure 5.* Temperature dependence of the surface residence time $\tau_{surf}$ of $NO_2$ interacting with $NH_4Cl$. The error bars indicate maximum and minimum values in separate experiments each using different $NH_4Cl$ coatings: ●; standard experiment, ○; large dose, □; aqueous solution coating, △; gas phase reaction.

of $NO_2$ with NaCl ($\gamma < 10^{-7}$) (Vogt and Finlayson, 1994; Fenter *et al.*, 1997a; Rossi, 2003).

Attempts to measure $\tau_{surf}$ for the interaction of $NO_2$ on solid NaCl substrates have been undertaken as an independent check. The value of $\tau_{surf}$ was found to be less than 2 $\mu$s because the arrival time spectra for $NO_2$ diffusing across the NaCl-coated tube in comparison with the reference tube was indistinguishable based on a 5% uncertainty in MS signal amplitude so that only this limiting value may be given. As far as the correlation between $\gamma$ and $\tau_{surf}$ goes the results for solid NaCl and $NH_4Cl$ are coherent: the extremely small value of $\gamma$ for NaCl correlates with an unmeasurably small value of $\tau_{surf}$ in contrast to the finite values for $NH_4Cl$ shown in Table I and Figures 5 and 6.

It is clear from the unusual temperature dependence of both $\gamma$ and $\tau_{surf}$ in the range 293–335 K that the reaction mechanism is complex as $\tau_{surf}$ shows positive temperature dependence from ambient to 323 K or negative temperature dependence when expressed as a rate constant. The present result is at variance with a study of $H_2O$ adsorption on soot using the same technique where a negative temperature dependence of $\tau_{surf}$ has been observed as expected (Alcala *et al.*, 2002). The negative temperature dependence of $1/\tau_{surf}$ which approximately amounts to $-8 \pm 2$ kcal mol$^{-1}$ ($-34 \pm 8$ kJ mol$^{-1}$) and the subsequent turnaround may be due to the occurrence of a complex uptake/reaction mechanism involving a two-channel reaction as presented in reactions (3) to (5). In addition, the unusual positive

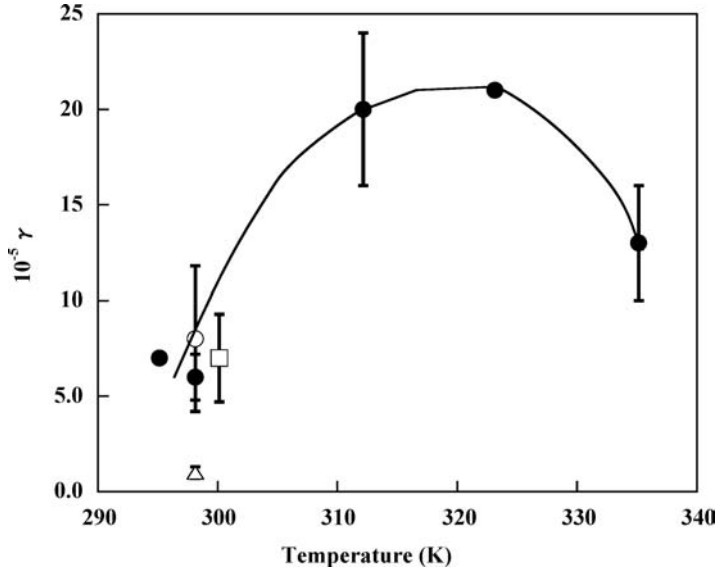


*Figure 6.* Temperature dependence of the uptake coefficient $\gamma$ of $NO_2$ interacting with $NH_4Cl$. The error bars indicate maximum and minimum values in separate experiments each using different $NH_4Cl$ coatings: ●; standard experiment, ○; high dose, □; aqueous solution coating, △; gas phase reaction.

temperature dependence of $\gamma$ up to 323 K displayed in Figure 6 corresponds to approximate activation energy of 11 $\pm$ 2 kcal mol$^{-1}$ (46 $\pm$ 8 kJ mol$^{-1}$). This result indicates that the gas phase reactant may be separated by significant barriers from both a non-reactive and a reactive surface intermediate leading to a stable reaction product of $NO_2$ with $NH_4Cl$. Figure 7 presents a sketch of a qualitative reaction energy (enthalpy) profile that is consistent with the significant positive and negative activation energy for $\gamma$ and $1/\tau_{surf}$, respectively. The increasing value of $\tau_{surf}$ with increasing temperature may be explained with the increasing population of the non-reactive and reactive surface intermediates, $NO_2$-$NH_4Cl$(s, NR) and $NO_2$-$NH_4Cl$(s, R) with temperature akin to a storage effect. The non-reactive intermediate $NO_2$-$NH_4Cl$(s, NR) must be stable with respect to the reactants $NO_2$ + $NH_4Cl$(s) so that it may function as a temporary reservoir for $NO_2$ at low temperature. This also holds for the reactive intermediate $NO_2$-$NH_4Cl$(s, R) as both assume the role of temporary holding tanks for $NO_2$. Figure 7 also explains the fact that the uptake coefficient increases with temperature at first and starts to decrease at the highest examined temperature. At low temperature the rate-limiting step is the crossing of the barrier to $NO_2$-$NH_4Cl$(s, R) that leads to an increasing rate of product formation with increasing temperature. At higher temperature the negative temperature dependence of $\gamma$ is explained by the fact that the dissociation of $NO_2$-$NH_4Cl$(s, R) back to reactants is favored over barrier crossing to products, essentially because of the nature of the transition states (loose for dissociation, tight for product formation).

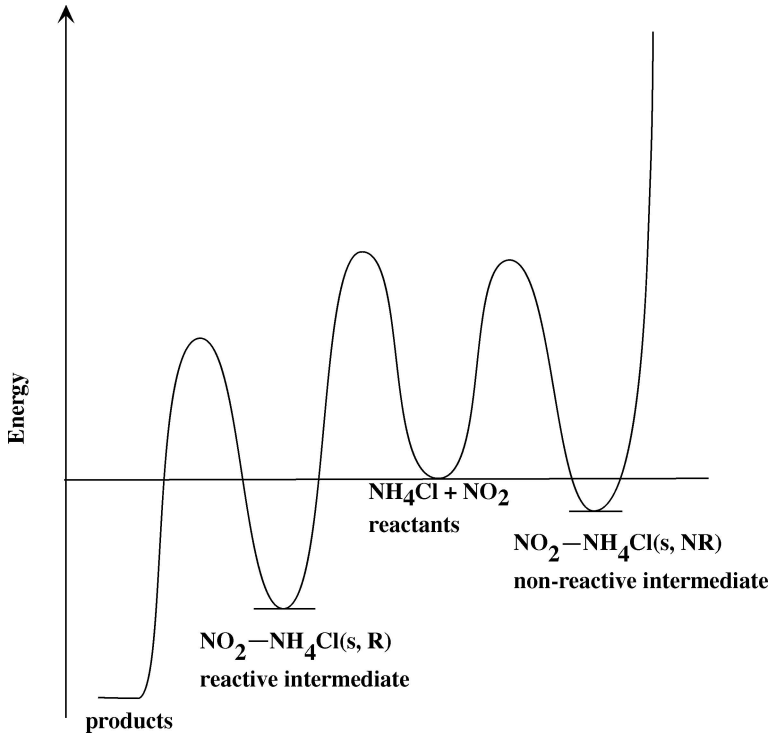


*Figure 7.* Qualitative reaction energy (enthalpy) profile of the heterogeneous reaction of $NO_2$ with solid $NH_4Cl$.

The essential feature of the mechanism is the fact that the formation of the non-reactive and reactive surface intermediate, $NO_2$-$NH_4Cl$(s, NR) and $NO_2$-$NH_4Cl$(s, R) do not lie on the same reaction coordinate which necessitates the existence of two corresponding surface sites on $NH_4Cl$. The surprise lies in the fact that both the reactive channel ($\gamma$) as well as the non-reactive channel ($\tau_{surf}$) are separated by significant barriers on the order of 8–11 kcal $mol^{-1}$ (34–46 kJ $mol^{-1}$) that may be equal within experimental uncertainty. At the highest temperature used in this study the trend of both $\gamma$ and $\tau_{surf}$ with temperature are reversing as shown in Figures 5 and 6 because the formation of stable products is competing with the formation of the non-reactive intermediate $NO_2$-$NH_4Cl$(s, NR) at the same time as the reactive intermediate $NO_2$-$NH_4Cl$(s, R) increasingly redissociates to reactants in agreement with the negative temperature dependence of $\gamma$. At the same time the surface residence time $\tau_{surf}$ decreases with temperature because of increasing competition from barrier crossing of the reactants towards products. Another way of expressing the decrease of $\gamma$ beyond 323 K is that of the two competing processes (−4) and (5) the former wins with increasing temperature starting at 323 K. This is a well known phenomenon in multichannel reactions and is related to the fact that the density of states (A-factor) atop the two reaction barriers is significantly

different. The mechanism is summarized below where g, s, R and NR denote gas phase, solid phase, reactive and non-reactive, respectively:

$$NO_2(g) + NH_4Cl(s) \rightleftharpoons NO_2\text{-}NH_4Cl(s, NR) \quad (3, -3)$$

$$NO_2(g) + NH_4Cl(s) \rightleftharpoons NO_2\text{-}NH_4Cl(s, R) \quad (4, -4)$$

$$NO_2\text{-}NH_4Cl(s, R) \rightarrow \text{products} \quad (5)$$

The reaction probability for a surface reaction that occurs according to a Langmuir–Hinshelwood mechanism is expected to increase with increasing surface residence time. This correlation has been shown using a few selected reactions for which both $\tau_{surf}$ and $\gamma$ have been determined using the diffusion tube for the determination of $\tau_{surf}$ and a low pressure reactor for $\gamma$ (Koch *et al.*, 1999). It simply states that "sticky" molecules have a larger reaction probability than non-sticky ones because they will indirectly hit a reactive surface site through adsorption and subsequent surface migration to a reactive site. Figure 8 shows a correlation between $\tau_{surf}$ and $\gamma$ measured at different temperatures but for the same reaction using data from Figures 5 and 6. One may notice that the data are roughly correlated when the considerable scatter in the individual values for $\tau_{surf}$ and $\gamma$ are taken into account. This correlation seems to hold also in the case of the present complex reaction mechanism.

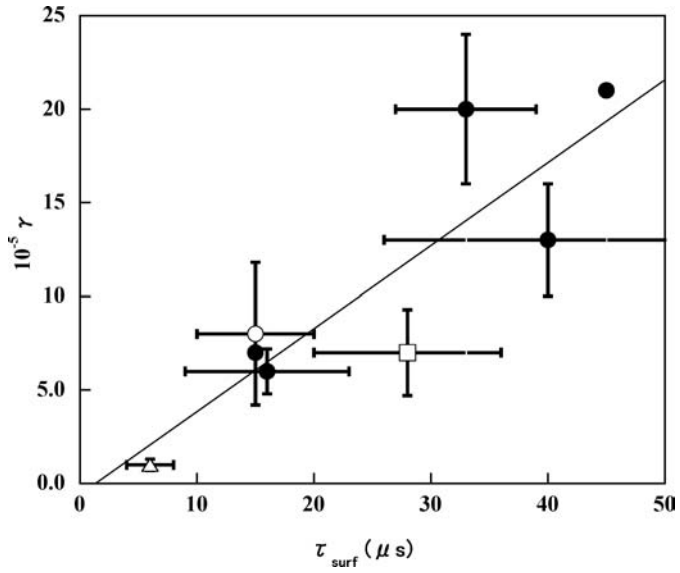


*Figure 8.* Relationship between the uptake coefficient $\gamma$ and the surface residence time $\tau_{surf}$. The error bars indicate maximum and minimum values in separate experiments each using different $NH_4Cl$ coatings: ●; standard experiment, ○; large dose, □; aqueous solution coating, △; gas phase reaction. $\gamma\ (10^{-5}) = 0.443 \times \tau_{surf}\ (\mu s) - 0.596$. The correlation coefficient is 0.87.

### 3.3. INFLUENCE OF THE COATING PROCEDURE ON THE KINETICS

Figures 5 and 6 show that the results for the large dose and the aqueous solution $NH_4Cl$-coating are very similar to the values obtained in standard experiments. However, both the values of $\tau_{surf}$ and $\gamma$ for the $NH_4Cl$-coating prepared from the gas phase neutralization reaction between HCl and $NH_3$ were significantly smaller compared to the standard experiment. The reason for this difference is not known as our experiments are not sensitive to the composition of the condensed phase. Experiments dealing with nucleation of solid $NH_4Cl$ from aqueous solutions do not point towards complications as far as the stable cubic crystal structure is concerned (Cohen *et al.*, 1987b). We tend to attribute the difference in reactivity and surface residence time to possible adsorption of $NH_3$ or HCl on $NH_4Cl$ because the flows to generate the $NH_4Cl$ aerosol were not quantitatively controlled, thus not strictly stoichiometric.

The uptake coefficient $\gamma$ and the surface residence time $\tau_{surf}$ of $NO_2$ on the $NH_4Cl$ coating prepared by gas phase neutralization of $NH_3$ and HCl and subsequent deposition of the aerosol on the internal surface of the diffusion tube are lower by a factor of 7 and 3.5, respectively, compared to the other preparation methods (see Table I). The $NH_4Cl$ salts in the environment are also produced by gas phase neutralization, although chemically different particles may initially serve as cloud condensation nuclei leading to cloud droplets (Young, 1993). However, the salt particles may deliquesce and grow into cloud droplets, but then may dry again depending on atmospheric conditions. For $NH_4Cl$ the deliquescence and efflorescence relative humidities are 79.5% and 45%, respectively (Cohen *et al.*, 1987a). In the atmosphere the number of cloud evaporation–condensation cycles is of the order of 10 before loss occurs through precipitation to the ground (Calvert, 1984; Seinfeld and Pandis, 1998). It becomes increasingly clear that many of the salt exchange reactions like the present one do not occur in the absence of adsorbed $H_2O$ and/or crystal imperfections. In order to clarify the difference in reactivity of $NO_2$ towards $NH_4Cl$-coatings that were prepared using different methods, particle surfaces have been investigated using scanning electron microscopy (SEM). Photographs 1 and 2 of Figure 9 show SEM images of $NH_4Cl$ films prepared by spraying a methanolic solution of $NH_4Cl$ and by deposition of the dry aerosol formed at atmospheric conditions, respectively. The deposited aerosol particles are spherical on the 10 $\mu$m scale and are smaller than those prepared by the methanol spray deposition which resemble those sprayed from an aqueous solution (not shown). According to these images (Figure 9) the internal surface of the deposited aerosol seems significantly larger than for the methanol spray. Nevertheless, the reactivity in terms of $\tau_{surf}$ and $\gamma$ of the latter is larger compared to the former as discussed above. The influence of the presence of $H_2O$ in the spray-coated films as well as crystal defects in the rapidly recrystallized film using the methanolic solution seems to be of major importance.

Figure 10 shows the dependence of the number of $NO_2$ pulses on the reaction probability in order to explore the saturation behavior of the $NH_4Cl$ substrate upon

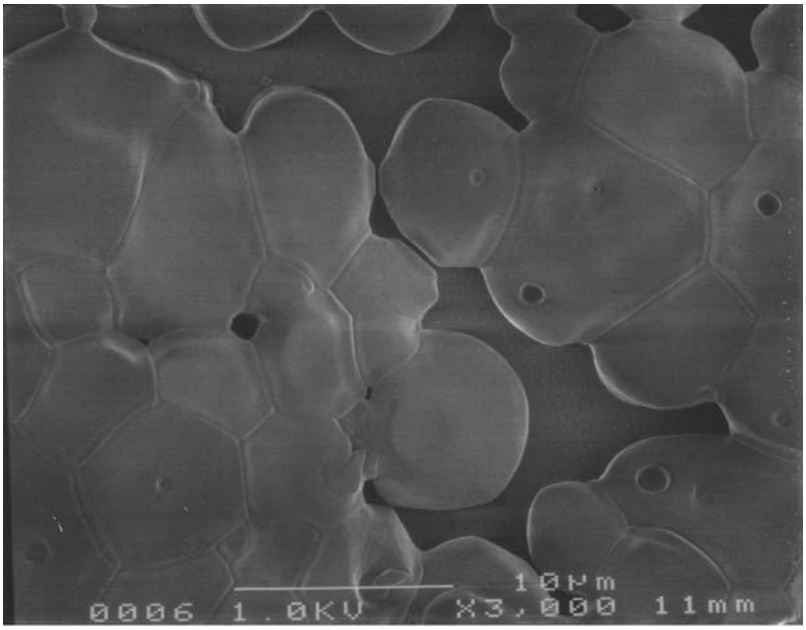


Photo 1 Methanol solution spray

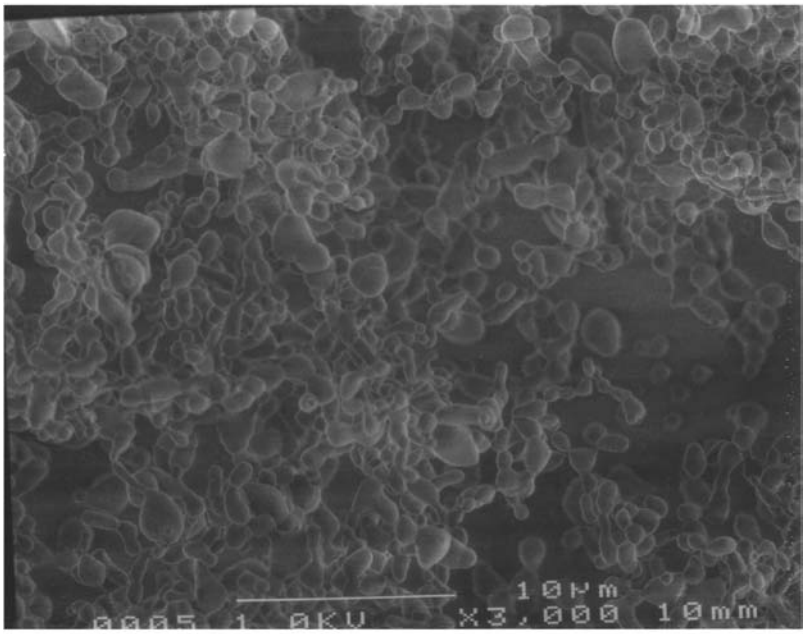


Photo 2 Gas phase preparation

*Figure 9.* SEM images of $NH_4Cl$ films sprayed onto glass supports. Photo 1: SEM image of $NH_4Cl$ film prepared by spraying a saturated methanol solution. A sprayed aqueous solution of $NH_4Cl$ resulted in an identical SEM image. Photo 2: SEM image of a $NH_4Cl$ film from deposition of dry aerosol formed at ambient pressure using the reaction $NH_3 + HCl$.

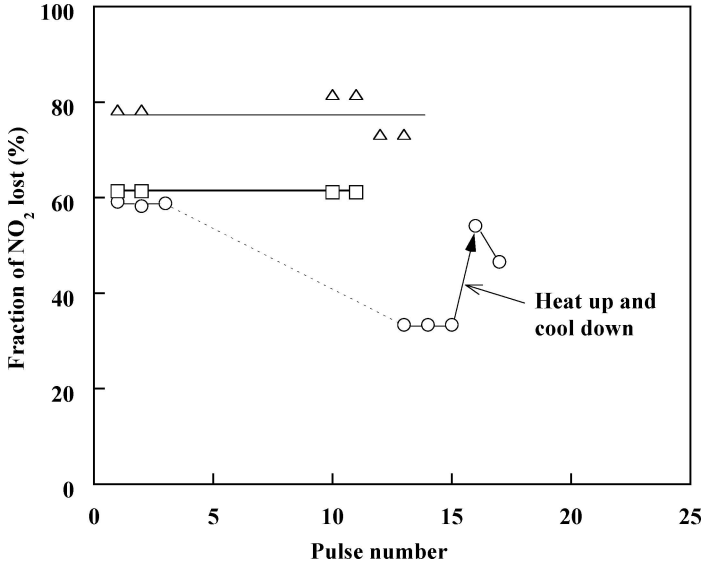


*Figure 10.* The relative number of $NO_2$ molecules per pulse disappearing through reaction with $NH_4Cl$ as a function of the cumulative number of pulses introduced at different temperatures. The number of molecules of $NO_2$ introduced per pulse was $4 \times 10^{14}$ molecules: ○; standard experiment at 298 K. The tube was heated to 423 K for 5 min after 15 pulses and cooled down. △; standard experiment at 312 K. □; standard experiment at 332 K.

repetitive dosing. At ambient temperature the initial reaction probabilities were roughly identical for the first few pulses, provided there was a sufficient quantity of salt adhering to the support. Figure 10 shows that $\gamma$ for a standard sample is already smaller by roughly a factor of two for the fifteenth pulse. Subsequently, the molecular diffusion tube was heated up to approximately 423 K for 5 min and then cooled down. The following interrogation with $NO_2$ pulses revealed a significant enhancement in $\gamma$ as displayed in Figure 10 to the original level. When the repetitive dosing experiments were carried out at higher temperature such as 312 K and 332 K no saturation effects were observed. The facile partial saturation of the $NH_4Cl$ substrate at ambient temperature points towards a limited number of active reaction centers on the salt substrate at any given time which may moreover depend on the coating procedure.

### 3.4. SATURATION EFFECTS AND REGENERATION

Using the data of Figure 10 we note that 60% of the first $NO_2$ pulse is disappearing through reaction and that 40% of the pulse of $4 \times 10^{14}$ molecules effuses which corresponds to an uptake coefficient of $\gamma \leq 10^{-4}$ according to Figure 4 and Table I. According to Figure 10 the relative reactive fraction of $NO_2$ drops to 30% with 70% of $NO_2$ effusing for the fifteenth pulse. The cumulative dose of $NO_2$ reacted giving rise to a 50% drop of reactive surface sites is therefore $8 \times 10^{12}$ molecule $cm^{-2}$ by

considering the partial saturation effect between the first and the fifteenth pulse and integrating the dose of $NO_2$ reacted on 361.3 $cm^2$ of $NH_4Cl$ substrate area. This integral reacted dose is put in relation with the total surface density of $6.7 \times 10^{14}$ formula units of $NH_4Cl$ per $cm^2$ of geometric surface that amounts to 1.2% of all possible reaction sites that disappear in 15 pulses. When we evaluate the number of reactive sites using $NO_2$ pulses of $4 \times 10^{15}$ molecules where the resolution of the saturation effect is lower we arrive at a number higher by a factor of 2.5, that is $2 \times 10^{13}$ molecule $cm^{-2}$. In conclusion, we arrive therefore at a typical reactive site density in the range 3.4–8.5 % for this specific salt substrate. The present results also point out that the saturation of active reaction sites on the substrate is reversible at higher than ambient temperature. A possible mechanism may be the surface migration of a solid albeit stable reaction product or its thermal decomposition (see below) thus freeing up the occupied reactive surface sites.

### 3.5. REACTION PRODUCTS AND ATMOSPHERIC IMPLICATIONS

All possible expected products were monitored as a function of time after admission of $NO_2$ into the diffusion tube. The only changes in intensity of the MS signals were observed at m/e = 47, 18 and 28. These correspond to the formation of HONO (m/e = 47), $H_2O$ (m/e = 18) and $N_2$ (m/e = 28) in the aftermath of a $NO_2$ pulse interacting with $NH_4Cl$. The quantitative results are shown in Table II where yields of observed products in percent relative to $NO_2$ reacted are shown. From the reaction products displayed in Table II the following reaction mechanism is proposed in reactions (4, −4), (5), (6) and (7):

$$NO_2(g) + NH_4Cl(s) \rightleftharpoons NO_2\text{-}NH_4Cl(s, R) \qquad (4, -4)$$

$$NO_2\text{-}NH_4Cl(s, R) + NO_2(g) \rightarrow NH_4NO_2(s) + NO_2Cl \qquad (5)$$

*Table II.* Products of the reaction of $NO_2$ on $NH_4Cl$

| | Ratio of product to $NO_2$ reacted (%) | | | | | |
|---|---|---|---|---|---|---|
| Temperature (°C) | $H_2O$ | $N_2$ | HONO | $H_2O/N_2$ | $HONO/N_2$ | Yield* |
| 298 | 16 | 5 | 35 | 3.4 | 7.3 | 0.80 |
| 298 | 6 | | 33 | | | |
| 312 | 3 | 2 | 51 | 1.8 | 29.5 | 1.06 |
| 312 | 4 | 2 | 63 | 1.5 | 26.0 | 1.31 |
| 314 | 5 | 2 | 31 | 2.4 | 14.7 | 0.66 |
| 332 | 3 | 1 | 54 | 2.8 | 55.9 | 1.10 |
| 335 | 23 | 9 | 64 | 2.7 | 7.5 | 1.45 |
| Average | | | | 2.4 | 23.5 | 1.06 |

*Ratio of the twice number of ($N_2$ + HONO) to the number of $NO_2$ reacted, $(2 \times ([N_2] + [HONO])/[NO_2])$.

$$NH_4NO_2(s) \rightarrow HONO(g) + NH_3(g) \quad (6)$$

$$NH_4NO_2(s) \rightarrow N_2(g) + 2H_2O(g) \quad (7)$$

The dominant products derived from the product MS spectrum and expected from the reaction mechanism described above are $NO_2Cl$, HONO and $NH_3$. Nitrylchloride, $NO_2Cl$, whose presence could not be confirmed using MS is expected to desorb into the gas phase but may perhaps also be adsorbed on $NH_4Cl$. Ammonia as a reaction product could not be identified because it contributes significantly to the mass spectral background owing to the thermal decomposition of the $NH_4Cl$ substrate. Nitrogen and water are expected products of the reaction of $NO_2$ with $NH_4Cl$ and have indeed been observed as decomposition products of $NH_4NO_2$. It is well known that $NH_4NO_2$ is very unstable and decomposes to $N_2$ and $H_2O$ (Rubin *et al.*, 1987). The average ratio of the yield of $H_2O$ relative to $N_2$ was $2.43 \pm 0.69$, close to the expected value of two within the measurement accuracy as displayed in Table II, column five. The branching ratio of reaction (6), redissociation of $NH_4NO_2$ into $NH_3$ and HONO, to reaction (7), thermal decomposition of thermally labile $NH_4NO_2$, is approximately 20 at ambient temperature and tends to increase with increasing temperature at the expense of the thermal decomposition, reaction (7). This conclusion is supported by the data of Table II, sixth column from the left, at the exception of data in rows one and five. Finally, data on the absolute yields of the sum of both pathways displayed in column 7 of Table II are in agreement with the increase of the uptake coefficient displayed in Table I.

The average uptake coefficient of $NO_2$ on $NH_4Cl$ is $7 \times 10^{-5}$ at 298 K, and more than 30% of $NO_2$ is transformed essentially quantitatively into HONO after diffusion across the sample tube. The heterogeneous reaction of $NO_2$ with ammonium salts may therefore be one of the sources of HONO in the atmosphere. Ammonium sulfate and ammonium nitrate are important ammonium salts in the atmosphere and are expected to react with $NO_2$ by the same mechanism, equations (8) and (9):

$$2NO_2(g) + NH_4HSO_4(s) \rightarrow NH_4NO_2(s) + NO_2HSO_4 \quad (8)$$

$$2NO_2(g) + NH_4NO_3(s) \rightarrow NH_4NO_2(s) + NO_2NO_3 \quad (9)$$

The title reaction may be compared to another heterogeneous reaction in which $NO_2$ reacts with NaCl or other alkali halides that are encountered in marine aerosols. Both reactions involve the loss of two moles of $NO_2$ per mole of $NH_4Cl$ or NaCl consumed. However, both reactions are found to be first order in $NO_2$ at such low pressures where the equilibrium fraction of $N_2O_4$ is negligible. Under these conditions the title reaction is at least 500 times faster compared to NaCl at identical substrate preparation procedures using spray coating and at similar crystalline morphology verified by SEM.

The reaction of $NO_2$ with ammonium salts could be a significant source of HONO in the atmosphere as the search continues for atmospheric sources of HONO that are heterogeneous in nature. The net reaction may be expressed in reaction (10) using the experimental first order rate law $r_{het} = k_{het}\,[NO_2] = \gamma\omega[NO_2]$ where

$k_{het}$ is the heterogeneous rate constant and $\omega$ is the collision frequency given by $\omega = (\langle c \rangle/4)S/V$ with S/V and $\langle c \rangle$ being the surface-to-volume ratio of the aerosol and the average molecular speed, respectively. Owing to the fact that $ClNO_2$ is formed as a reaction product that rapidly undergoes photolysis leading back to $NO_2 + Cl$ the net reaction effectively

$$2NO_2 + NH_4Cl \rightarrow ClNO_2 + NH_3 + HONO \quad (10)$$

consumes just one mole of $NO_2$ which is reduced to HONO with simultaneous oxidation of chloride to atomic Cl. Ammonium salts occur in two size classes in the aerosol fine fraction ($PM_{2.5}$), namely the condensation and accumulation mode with a diameter of 0.2 and 0.7 $\mu$m (Wall *et al.*, 1988; Seinfeld and Pandis, 1998). If we assume a mass loading of 150 $\mu g\ m^{-3}$ as an upper limit that is exclusively centered on the condensation and the droplet mode, we obtain a S/V ratio of $3 \times 10^{-5}$ and $8.6 \times 10^{-6}\ cm^2\ cm^{-3}$, respectively, with a particle number concentration of $2.4 \times 10^4$ and 560 particles $cm^{-3}$, respectively, assuming $\rho = 1.5\ g\ cm^{-3}$. This assumption, while admittedly representing a limiting case, leads to a heterogeneous rate coefficient $k_{het}$ of $2.5 \times 10^{-5}$ and $8 \times 10^{-6}\ s^{-1}$ corresponding to a $NO_2$ lifetime of 10 and 34 h for the condensation and accumulation mode, respectively. The rate constant for mass transfer of $NO_2$ towards the aerosol surface is a factor of 3000 to $10^4$ faster than the heterogeneous reaction so that it does not need to be considered here. In case the mass loading is reduced by a factor of ten all parameters scale linearly leading to a decrease of $k_{het}$ by an order of magnitude. This result shows that the title reaction may be significant under certain atmospheric conditions.

A comparison of the heterogeneous HONO rate of formation with its homogeneous counterpart is instructive and leads to the same conclusion: using a rate constant of $7.4 \times 10^{-12}\ cm^3\ s^{-1}$ for the reaction OH + NO → HONO at 1 atmosphere a homogeneous rate of HONO formation of $7 \times 10^6\ s^{-1}\ cm^{-3}$ is found compared to the heterogeneous rate of $2.7 \times 10^7\ s^{-1}\ cm^{-3}$ for [NO] and [$NO_2$] equal to 20 and 40 ppb, respectively, and [OH] = $2 \times 10^6\ cm^{-3}$. This shows that the homogeneous and the heterogeneous rates are of comparable magnitude under the chosen conditions. If $NO_2$ were to react with dry-deposited ammonium salts on the ground the rate of HONO formation would most likely be significantly larger owing to the expected larger value of S/V compared to ammonium salt aerosols.

## Acknowledgement

This study has been supported in part by Grant-in-Aid for Scientific Research (C) (KAKENHI 13680608) from Japan Society for the Promotion of Science as well as by the AVINA Foundation in the framework of the Alliance of Global Sustainability (AGS), project "Regional Air Quality and Climate Change." This work was performed at LPAS/EPFL.

## References


Alcala-Jornod, C. and Rossi, M. J., 2000: Reactivity of $NO_2$ and $H_2O$ on soot generated in the laboratory from a diffusion flame, *Phys. Chem. Chem. Phys.* **2**, 5584–5593.

Alcala-Jornod, C., van den Bergh, H., and Rossi, M. J., 2002: Can soot particles emitted by airplane exhaust contribute to the formation of aviation contrails and cirrus clouds? *Geophys. Res. Lett.* **29**(17), 1820, doi:10.1029/2001GL014115.

Alcala-Jornod, C. and Rossi, M. J., 2004: The chemical kinetics of the interaction of $H_2O$ vapor with soot in the range $190 \leq T/K \leq 300$: A diffusion tube study, *J. Phys. Chem. A* **108**, 10667–10680.

Ammann, M., Kalberer, M., Jost, D. T., Tobler, L., Rössler, E., Piguet, D., Gäggeler, H. W., and Baltensperger, U., 1998: Heterogeneous production of nitrous acid on soot in polluted air masses, *Nature* **395**, 157–160.

Baum, M. M., Kiyomiya, E. S., Kumar, S., Lappas, A. M., Kapinus, V. A., and Lord, H. C., 2001: Multicomponent remote sensing of vehicle exhaust by dispersive absorption spectroscopy. 2. Direct on-road ammonia measurements, *Environ. Sci. Technol.* **35**, 3735–3741.

Boudart, M. and Djéga-Mariadassou, G., 1984: Kinetics of heterogeneous catalytic reactions, Princeton University Press, Princeton, N. J. (USA), ch. 2.

Bouwman, A. F., Lee, D. S., Asman, W. A. H., Dentener, F. J., van der Hoek, K. W., and Olivier, J. G. J., 1997: A global high-resolution emission inventory for ammonia, *Global Biogeochem. Cycles* **11**, 561–587.

Calvert, J. G., 1984: *$SO_2$, NO and $NO_2$ Oxidation Mechanisms: Atmospheric Considerations*, Butterworth Publishers, Boston, ch. 5.

Cohen, M. D., Flagan, R. C., and Seinfeld, J. H., 1987a: Studies of concentrated electrolyte solutions using the electrodynamic balance. 1. Water activities for single-electrolyte solutions, *J. Phys. Chem*. **91**, 4563–4574.

Cohen, M. D., Flagan, R. C., and Seinfeld, J. H., 1987b: Studies of concentrated electrolyte solutions using the electrodynamic balance. 3. Solute nucleation, *J. Phys. Chem*. **91**, 4583–4590.

DeMore, W. B. *et al.*, 1997: *Chemical Kinetics and Photochemical Data for Use in Stratospheric Modeling*, NASA, 12, p.142.

Fehsenfeld, F. C., Huey, L. G., Leibrock, E., Dissly, R., Williams, E., Ryerson, T. B., Norton, R., Sueper, D. T., and Hartsell, B., 2002: Results from an informal intercomparison of ammonia measurement techniques, *J. Geophys. Res.* **107**(D24), doi:10.1029/2001JD001327, 2002.

Fenter, F. F., Caloz, F., and Rossi, M. J., 1997a: Paper I: Design and construction of a Knudsen-cell reactor for the study of heterogeneous reactions over the temperature range 130–750 K: Performances and Limitations, *Rev. Sci. Instrum.* **68**, 3172–3179.

Fenter, F. F., Caloz, F., and Rossi, M. J., 1997b: Paper II: Simulation of flow conditions in low-pressure flow reactors (Knudsen cells) using a Monte Carlo technique, *Rev. Sci. Instrum.* **68**, 3180–3186.

Finlayson-Pitts, B. and Pitts, Jr. J. N., 1999: *Chemisty of the Upper and Lower Atmosphere*, Academic Press, p. 574.

Fraser, M. P. and Cass, G. R., 1998: Detection of excess ammonia emissions from in-use vehicles and the implications for fine particle control, *Environ. Sci. Technol*. **32**, 1053–1057.

Grassian, V. H., 2001: Heterogeneous uptake and reaction of nitrogen oxides and volatile organic compounds on the surface of atmospheric particles including oxides, carbonates, soot and mineral dust: Implications for the chemical balance of the troposphere, *Int. Rev. Phys. Chem.* **20**, 467–548.

Henning, S., Weingartner, E., Schwikowski, M., Gäggeler, H. W., Gehrig, R., Hinz, K.-P., Trimborn, A., Spengler, B., and Baltensperger, U., 2003: Seasonal variation of water-soluble ions of the aerosol at the high-alpine site Jungfraujoch (3580 m asl), *J. Geophys. Res*. **108**, 4030, doi:10.1029/2002DJ002439.

Huygen, I. C., 1971: Reaction of nitrogen dioxide with Griess type reagent, *Anal. Chem.* **42**, 407–409.

Jacobson, M. Z., 2001: Global direct radiative forcing due to multicomponent anthropogenic and natural aerosols, *J. Geophys. Res.* **106D**, 1551–1568.

Koch, T. G., Fenter, F. F., and Rossi, M. J., 1997: Real-time measurement of residence times of gas molecules on solid surfaces, *Chem. Phys. Lett.* **275**, 253–260.

Koch, T. G. and Rossi, M. J., 1998: Direct measurement of surface residence times: Nitryl chloride and chlorine nitrate on alkali halides at room temperature, *J. Phys. Chem.* **102A**, 9193–9201.

Koch, T. G., van den Bergh, H., and Rossi, M. J., 1999: A molecular diffusion tube study of $N_2O_5$ and $HONO_2$ interacting with NaCl and KBr at ambient temperature, *Phys. Chem. Chem. Phys.* **1**, 2687–2694.

Levaggi, D. A., Siu, W., and Feldstein, M., 1973: A new method for measuring average 24-hour nitrogen dioxide concentrations in the atmosphere, *J. Air Poll. Control Assoc.* **23**, 30–33.

Longfellow, C. A., Ravishankara, A. R., and Hanson, D. R., 1999: Reactive uptake on hydrocarbon soot: Focus on $NO_2$, *J. Geophys. Res.* **104**, 13833–13840.

Markwalder, B., Gozel, P., and van den Bergh, H., 1992: Temperature-jump measurements on the kinetics of association and dissociation in weakly bound systems: $N_2O_4 + M = NO_2 + NO_2 + M$, *J. Chem. Phys*. **97**, 5472–5479.

Puteaud, J.-P. *et al.*, 2002: An European aerosol phenomenology; physical and chemical characteristics of particulate matter at kerbside, urban, rural and background sites in Europe, European Commission, Report no. EUR 20411 EN (http://ies.jrc.cec.eu.int/Download/cc).

Rossi, M. J., 2003: Heterogeneous reactions on salt, *Chem. Rev.* **103**, 4823–4882.

Rubin, M. B., Noyes, R. M., and Smith, K. W., 1987: Gas-evolution oscillators. 9. A study of the ammonium nitrite oscillator, *J. Phys. Chem.* **91**, 1618–1622.

Seinfeld, J. H. and Pandis, S. N., 1998: *Atmospheric Chemistry and Physics,* John Wiley & Sons, Inc, pp. 529–533 and pp. 589–591.

Tabor, K., Gutzwiller, L., and Rossi, M. J., 1994: Heterogeneous chemical kinetics of $NO_2$ on amorphous carbon at ambient temperature, *J. Phys. Chem.* **98**, 6172–6186.

Tseng, C. H. and Keener, T. C., 2001: Enhanced effect of in-situ generated ammonium salt aerosols on the removal of $NO_x$ from simulated flue gas, *Environ. Sci. Technol.* **35**, 3219–3224.

Underwood, G. M., Song, C. H., Phadnis, M., Carmichael, G. R., and Grassian, V. H., 2001: Heterogeneous reactions of $NO_2$ and $HNO_3$ on oxides and mineral dust: A combined laboratory and modeling study, *J. Geophys. Res*. **106D**, 18055–18066.

Van Veldhuizen, E. M., Zhou, L. M., and Rutgers, W. R., 1998: Combined effects of pulsed discharge removal of NO, $SO_2$ and $NH_3$ from flue gas, *Plasma Chem. Plasma Proc.* **18**, 91–111.

Vogt, R. and Finlayson-Pitts, B., 1994: A diffuse-reflectance infrared fourier-transform spectroscopic (DRIFT) study of the surface-reaction of NaCl with gaseous $NO_2$ and $HNO_3$., *J. Phys. Chem.* **98**, 3747–3775.

Wall, S. M., John, W., and Ondo, J. L., 1988: Measurement of aerosol size distributions for nitrate and major ionic species, *Atmos. Environ.* **22**, 1649–1656.

Weis, D. D. and Ewing, G. E., 1999: The reaction of nitrogen dioxide with sea salt aerosol, *J. Phys. Chem.* **103A**, 4865–4873.

Young, K. C., 1993: *Microphysical Processes in Clouds,* Oxford University Press, pp. 57–62.